

# Design of Monolithic RF CMOS Sub-mW Self-Oscillating-Mixers

S. FENNI<sup>1,2</sup>, F. HADDAD<sup>1</sup>, A. SLIMANE<sup>3</sup>, R. TOUHAMI<sup>2</sup>, W. RAHAJANDRAIBE<sup>1</sup>

<sup>1</sup> Aix Marseille Université, CNRS, Université de Toulon, IM2NP UMR 7334, 13397, Marseille, FRANCE

<sup>2</sup> USTHB University, Instrumentation Laboratory LINS, Algiers, ALGERIA

<sup>3</sup> DMN, Centre de développement des technologies avancées, Baba Hassan, Algiers, ALGERIA

**Abstract:** —In this paper, different topologies of RF self-oscillating mixers (SOM), stacking the voltage controlled oscillator (VCO) and the mixer on top of each other, are assessed. Their design considerations to address sub-mW operation suitable to ultra-low power applications are presented. Two configurations of SOM circuits are implemented in 130nm CMOS technology. The obtained results are presented and performances in terms of gain, noise, linearity, area, power consumption and stability over process and mismatch are compared and discussed.

**Keywords:** - RF; SOM; LC-VCO; mixer; CMOS.

Received: April 12, 2022. Revised: February 18, 2023. Accepted: March 13, 2023. Published: April 21, 2023.

## 1. Introduction

The emergence of the Internet of Things (IoT) leads to stringent requirements on the power consumption of devices. The energy budget is restricted because of the limited battery lifetime and the unstable output power of energy harvesters. This rapidly became a key issue driving the implementation of ultra-low power (ULP) radiofrequency (RF) integrated circuits (IC). To reduce power consumption, several techniques are used in RF design: lowering either the supply voltage or the current. First, low voltage operation can be achieved when RF front-ends in transceivers use folded topologies. The stacked circuit is converted to a cascaded one and then voltage and power consumption are reduced [1]. Besides, lowering the current can be achieved with current-reuse technique in the RF front-end. The overall power consumption is reduced since the bias current is shared between multiple blocks stacked one on top of the other. Many examples of current reuse configurations are proposed in literature. [2] presents a voltage controlled oscillator (VCO) using NMOS and PMOS pairs that share the available current and leads to an equivalent transconductance as standard cross-coupled topology but consuming half of the power.

Another efficient approach is to combine different functions of the RF front-end in a single circuit sharing the current [3]. Merging the low-noise amplifier (LNA) and the VCO has been proposed in [4] and depicts ultra-low power consumption for wireless sensor network applications. Also, the LNA and the mixer have been combined in one circuit achieving a good conversion gain and low power consumption despite of high noise factor [5], [6]. Another combination is between the VCO and the mixer called self-oscillating mixer (SOM) (Fig. 1) [7], [8].

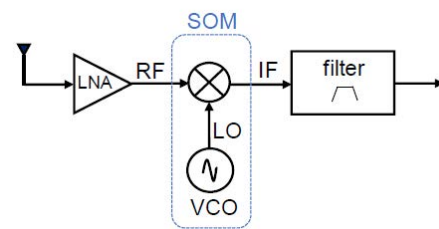


Fig. 1. Block diagram of RF front-end receiver using a SOM

In some configurations, low noise amplification is added to the SOM resulting in LMV (LNA-Mixer-VCO) circuit [9], [10]. The SOM based topologies are good candidate for ULP and low-cost applications. But, great design considerations should be taken into account since dynamics and performances of the combined building blocks have mutual dependencies [11].

In this paper, different topologies of self-oscillating mixers have been implemented and compared. Hence, depending on the design constraint, this work can help designers to choose the suitable architecture of the circuit. Section II depicts both configurations of SOM circuits and their operating principle. The proposed designs are presented in section III, while the obtained results are discussed in section IV. Conclusions are given in section V.

## 2. Self-oscillating mixer topologies

The principle of SOMs is based on merging the mixer and the local oscillator (LO) on one circuit. Thus, the dc bias current is reused which decreases their power consumption compared to the conventional cascaded mixer and oscillator circuits. The first designer's constraint is to choose the most appropriate topology for the SOM. That is led by the type and the disposition of the used blocks.

Concerning the oscillator, LC-VCO is recommended since it consumes less power for a given phase noise requirement. The LC-tank determines the frequency while the active cross-coupled pair allows the LC-tank loss cancellation to sustain the oscillations [12]. Concerning the mixer, Gilbert active cells are usually used in SOM circuits. They consist of a transconductor stage, ensuring the voltage-to-current conversion, and an on/off

switching core resulting in an intermediate frequency (IF) signal. Despite their low noise figure (NF), they have high linearity, high voltage conversion gain (VCG) and large frequency response [13], [14], [15], [16]. Their NF can be improved by adding some design noise reduction techniques [17].

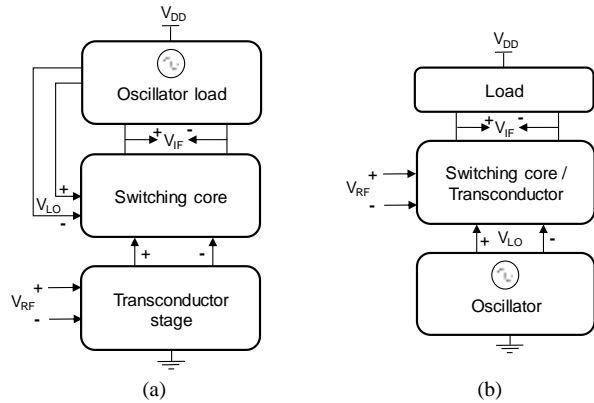


Fig. 2. SOM topologies : (a) Config1 : the oscillator is stacked above the mixer and (b) Config2: the oscillator is below the RF input stage

Most SOM topologies in literature are based on the configurations shown in Fig.2, that we will denote Config1 and Config2. In Config1 based SOMs, the oscillator is stacked above the mixer which is led by an RF transconductor stage, as depicted in Fig. 2(a). The RF input signal ( $V_{RF}$ ) is applied into the transconductor stage of the Gilbert mixer. The resulting signal is multiplied with the LO signal ( $V_{LO}$ ) applied to the switching core, and then the obtained IF current is converted through the load to an IF voltage ( $V_{IF}$ ) [10], [18], [19]. In Config2 based SOMs, the oscillator is below the mixer, as shown in Fig. 2(b). The LO and RF inputs are injected into the switching core. In this case, the more appropriate mixing topology is the commuting mixer in which one stage of transistors can be used simultaneously as transconductance and as switches [20], [21].

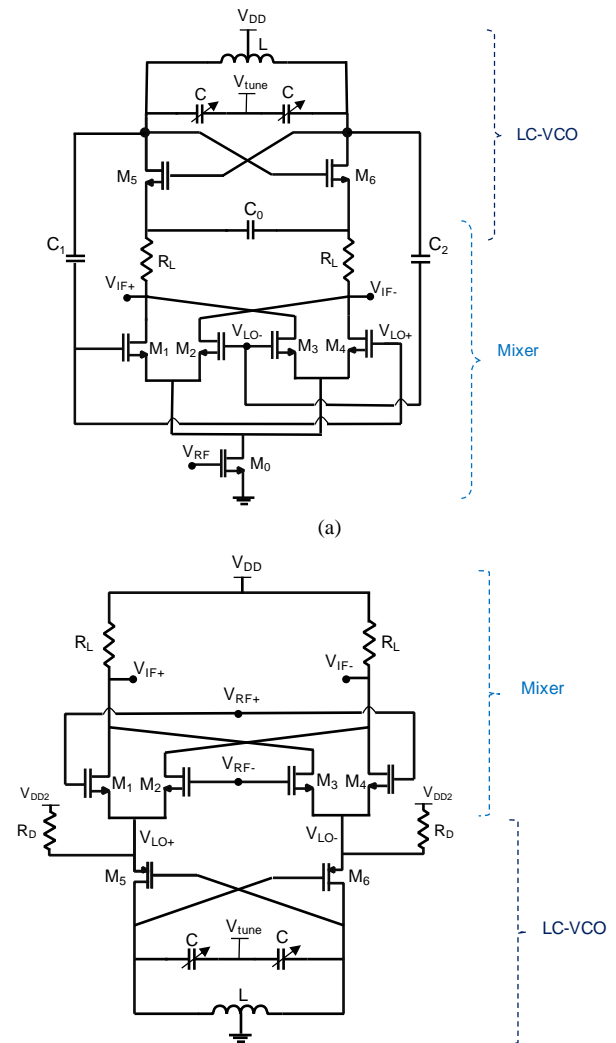
### 3. Self-oscillating mixer designs

Two SOM circuits based on the configurations discussed above have been implemented in 130nm CMOS technology to compare their performances and to discuss the suitable choices according to a given design specification. Fig. 3 shows the schematics of the proposed self-oscillating mixers. Those SOM circuits have been designed to work at 2.4GHz, a frequency band suitable to many wireless communication standards such as Wi-Fi, Bluetooth, ZigBee, etc.

In Config1 SOM, shown in Fig. 3(a), the LC-VCO, that generates the oscillations, is stacked above a double-balanced mixer. The NMOS cross-coupled pair  $M_5$ - $M_6$  are used for the oscillator, while  $M_1$ - $M_4$  constitute the switching core for the mixer. Capacitor  $C_0$  gives a path for LO signal which drives  $M_1$ - $M_4$  via capacitors  $C_1$  and  $C_2$  to achieve the current switching function. In the 1<sup>st</sup> half LO period,  $M_1$ ,  $M_4$  and  $M_5$  are ON, thus output RF current of  $M_0$  flows into them through the load  $R_L$  and  $C_0$ , while  $M_2$ ,  $M_3$  and  $M_6$  are OFF, resulting in an IF current. In the 2<sup>nd</sup> half period,  $M_2$ ,  $M_3$  and  $M_6$  are ON and the current flows through them, achieving a complementary

operation with a resulting IF current. The differential current is converted by the resistive loads into an output IF voltage. Therefore, the cross-coupled pair of the VCO,  $M_5$ - $M_6$ , contributes to the switching function without perturbing the natural operation of the mixer. Transistor  $M_0$  acts as a transconductance (gm) and as a tail current to adjust the dc bias in the circuit.

In the proposed Config2 SOM, shown in Fig. 3(b), the LC-VCO uses a PMOS cross-coupled pair ( $M_5$ - $M_6$ ) for tank loss compensation instead of NMOS pairs as usually used in literature [20]. In fact, since the mixer ( $M_1$ - $M_4$ ) is stacked above the VCO, the mixer bloc appears as an external load for the VCO. Here, the output LO signals are chosen to be at the sources of the PMOS cross-coupled pair, instead of their drains in the NMOS version, in order to isolate the resonator from any load effect. Thus, the loading problem can be avoided which improves the quality factor and the phase noise (PN) performances [22]. The RF signal is applied to the gates of the transistors ( $M_1$ - $M_4$ ) that are switched ON/OFF by the LO signal fed into their sources. A further supply voltage  $V_{dd2}$  is added to the LC-VCO section, via resistors  $R_D$ , in order to provide more dc current and to reduce the dependence between both SOM blocks improving the circuit performance.



(b)

Fig. 3. Proposed (a) Config1 and (b) Config2 self-oscillating mixer schematics

The voltage conversion gain of the circuit depends essentially on the transconductance value. It can be expressed as

$$VCG \approx \frac{1}{2} g_m R \quad (1)$$

where  $g_m$  is equal to  $g_{m0}$  (transconductance of transistor  $M_0$ ) and to  $g_{m1-4}$  (transconductance of transistors  $M_1$ - $M_4$ ) in Config1 and Config2 SOMs, respectively. Concerning R, it is equal to  $R_x//R_L$  and to  $R_L$  in Config1 and Config2 SOMs, respectively.  $R_x$  is the resistance seen at the sources of  $M_5$  and  $M_6$ . It highly depends on the equivalent resistance of the LC tank and its quality factor. Since this resistance tends to be small, it causes the decrease of the conversion gain, which is one of the limitations of this structure. Also, the load charge  $R_L$  cannot be highly increased because of the limited voltage headroom given by the supply voltage, given in (2). Only a certain dc voltage  $V_{Rmax}$  across it is allowed, corresponding to a maximum resistance value  $R_{Lmax}$ .

$$V_{DD} \approx V_{od_0} + V_{od_{1,2}} + V_{GS_{3,4}} + V_{Rmax} \quad (2)$$

where  $V_{od_i}$  denote the overdrive voltage ( $V_{GS_i} - V_{th_i}$ ) of the transistor  $M_i$ , and  $V_{Rmax} = I_{D0} R_{Lmax}$ .

One of SOM circuit design challenges is to judiciously size the transconductance  $g_m$  in the mixer section since it has a direct impact on the voltage conversion gain. In Config1 SOM, the conversion gain depends on the dc current  $I_{D0}$  across  $g_{m0}$  which is limited for a fixed power budget, constraining the choice of  $g_{m0}$ . That can be expressed as

$$g_{m0} = \mu_n C_{ox} \frac{W_0}{L_0} (V_{GS0} - V_{th}) \quad (3)$$

where  $W_0$ ,  $L_0$  and  $V_{GS0}$  are the width, length, gate-to-source voltage of transistor  $M_0$ , respectively.  $V_{th}$  is the threshold voltage.

In Config2 SOM, the transconductance depends on the LO signal injected to their sources. Transistors  $M_1$ - $M_4$  are switched ON/OFF according to  $V_{LO}$  variation. Considering  $V_{LO,dc}$  as the dc voltage and  $V_{LO,OFF}$  as the minimum value of  $V_{LO}$  turning OFF the transistors  $M_1$ - $M_4$ , the operating principle of the proposed SOM is shown in Fig. 4. When  $V_{LO} < V_{LO,dc}$ , transistors are ON providing a certain value of  $g_m$ . While  $V_{LO}$  increases,  $g_m$  decreases until it is OFF for  $V_{LO} \geq V_{LO,OFF}$ . This latter can be expressed as

$$V_{LO,OFF} = V_{G1-4} - V_{th} \quad (4)$$

where  $V_{G1-4}$  is the gate voltage of transistors  $M_1$ - $M_4$ .

The switched transconductance of  $M_1$ - $M_4$  has the following expression

$$\begin{aligned} g_{m1-4} &= \mu_n C_{ox} \left( \frac{W}{L} \right)_{1-4} (V_{LO,OFF} - V_m) \\ &= \mu_n C_{ox} \left( \frac{W}{L} \right)_{1-4} (V_{GS1-4} - V_{LO,dc} - V_{th} - V_m) \end{aligned} \quad (5)$$

where  $V_{GS1-4}$  and  $V_m$  are the gate-to-source voltage and the magnitude of  $V_{LO}$ , respectively.  $W_{1-4}$  and  $L_{1-4}$  are the width and length of transistors  $M_1$ - $M_4$ , respectively.

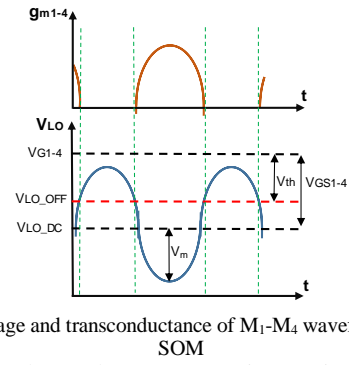


Fig. 4. LO voltage and transconductance of  $M_1$ - $M_4$  waveforms in Config2 SOM

As a result, the voltage conversion gains of both SOM structures can be expressed as

$$VCG_{Config1} \approx \frac{1}{2} \mu_n C_{ox} \frac{W_0}{L_0} (R_x//R_L) (V_{GS0} - V_{th}) \quad (6)$$

$$VCG_{Config2} \approx \frac{1}{2} \mu_n C_{ox} \frac{W_{1-4}}{L_{1-4}} R_L (V_{GS1-4} - V_{LO,dc} - V_{th} - V_m) \quad (7)$$

In order to increase the conversion gain, it is necessary to increase either the resistor or the transconductance values. Nevertheless, they are limited by the voltage headroom, that can also affect the power consumption and the noise contribution in the mixer [23]. Thus a design tradeoff between these performances should be taken into account. Furthermore, the noise at the IF output can be considered as the addition of the single noise contributions of the different sections of the self-oscillating mixer. In order to improve the noise performance of the SOM, the switching transistors need to be biased at a low dc current which decreases the 1/f noise portion. In Config1 SOM, since both stages formed by  $M_0$  and ( $M_1$ - $M_4$ ) share the same DC current, the linearity of the transconductance stage is affected. Hence, another design tradeoff between noise and linearity in SOM circuits should be taken into account, while maintaining the same oscillation frequency.

## 4. Self-oscillating mixer results

Both SOM configurations, shown in Fig. 3, are implemented in 130nm CMOS technology to limit the cost of the RF front-end. Their oscillation frequency is calibrated to be on the 2.4GHz ISM band and can be tuned by changing the voltage  $V_{tune}$ . Transistors are sized to work with a regular voltage threshold, and supply voltage is 1.2V ( $V_{DD2}$  is equal to 0.6V). Both self-oscillating mixers allow reaching sub-mW operation. Their power consumptions are 800 $\mu$ W and 600 $\mu$ W for Config1 and Config2 SOMs, respectively.

Knowing that inductor is the biggest component in RF devices, and since only one inductor is used on both proposed SOM circuits, the occupied areas of Config1 and Config2 are similar and equal to 0.24mm<sup>2</sup>.

The obtained conversion gains are shown in Fig. 5. The LO signal has been tuned through  $V_{tune}$  in order to get the performances at different IF frequencies. It can be seen that Config1 SOM performs a higher conversion gain than Config2 SOM. It is around 18dB for Config1 versus 9dB for Config2.

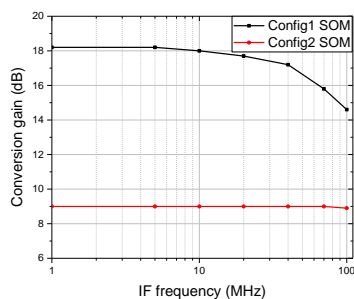


Fig. 5. Conversion gain of both SOM configurations

Moreover, Fig. 6 shows the obtained phase noise profiles of both circuits. It can be noticed that a phase noise of -113dBc/Hz and -110dBc/Hz at 1MHz offset frequency for Config1 and Config2 SOMs, respectively. This result is as expected from the previous section. While maintaining a comparable current to sustain oscillations and then a comparable power consumption between both structures, the VCG is better in the first configuration.

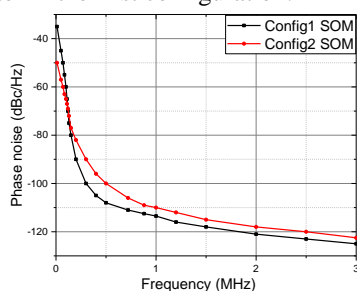


Fig. 6. Phase noise of both SOM configurations

Noise and gain performances of the Config1 are better than Config2 because of the transconductance  $g_{m0}$  that addresses a part of low noise amplification function too.

Generally, the linearity is poor in SOM circuits, since the mixer is biased at a low dc current. For example, in Config1 topology, the 3<sup>rd</sup> order intercept point (IIP3) can be approximated as [24]

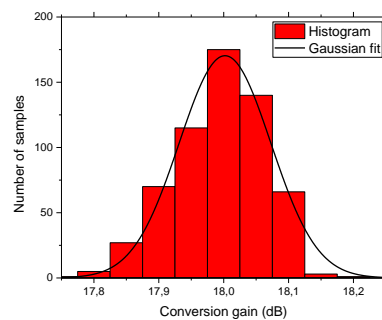
$$IIP3 = \sqrt{\frac{4}{3} \left| \frac{g_{m0}}{K3g_{m0}} \right| f_1 f_2 C_{gs0}} \quad (8)$$

where  $C_{gs0}$  is the parasitic gate to source capacitance of transistor  $M_0$  and  $K3g_{m0}$  is the second derivative of the small signal transconductance with respect to an input voltage with input frequencies  $f_1$  and  $f_2$  in a 2-tone test. Hence, by reducing the dc current,  $g_{m0}$  decreases which results in a low linearity. In the proposed Config1 SOM, the obtained IIP3 is -4dBm. The main source of distortion in Config2 SOM is the non-linearity of transistors  $M_1$ - $M_4$ . The larger these transistors are, the higher is their IIP3. Also, increasing the overdrive voltage of  $M_1$ - $M_4$  can improve the linearity of the mixer at the cost of a higher power consumption. The obtained IIP3 is -12dBm for Config2 SOM.

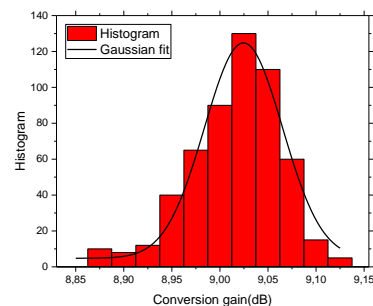
Besides, the device and process mismatch analysis for the proposed self-oscillating mixers has been carried out by Monte Carlo simulations. The performed 600 runs include random variations of process and device mismatch. The illustrated histograms on Fig. 7 give the obtained conversion gain at an IF frequency of 10 MHz from an RF frequency of 2.45GHz. It can be noticed that both configurations have very narrow

spread showing the gain stability of these SOMs versus process and mismatch uncertainties. Their standard deviations are equal to 0.003 and 0.002 with  $\sigma$  of 0.07 and 0.04 through mean values of 18dB and 9dB for Config1 and Config2, respectively.

A performance summary and comparison of the proposed SOM circuits with other published works is shown in Table 1.



(a)



(b)

Fig. 7. Monte Carlo analysis of the conversion gain for (a) Config1 and (b) Config2 SOMs

	This work		[18]	[20]	[25]
	Config1	Config2	Config1	Config2	Config1
CMOS process (nm)	130	130	130	180	65
RF frequency (GHz)	2.45	2.45	7.8-8.8	4.2	2.5
IF frequency (MHz)	10	10	300	55	7
Supply voltage (V)	1.2	1.2	1.5	1	1
Conversion gain (dB)	18	9	11.6	10.9	10
PN @1MHz (dBc/Hz)	-113	-110	-102	-113.1	-107.4
Power $P_{dc}$ (mW)	0.8	0.6	12	3.14	0.6
IIP3 (dBm)	-4	-12	-8.3	-11.8	-
Area (mm <sup>2</sup> )	0.24	0.24	0.47	0.96 *	1.2 *

\*with pads

## 5. Conclusion

Two configurations of monolithic self-oscillating mixers have been presented and designed in this paper in CMOS process. A comparative study of their performances has also been carried out. By adopting a SOM approach, stacking the mixer and the VCO on top of each other, it is shown that the area and the power consumption are reduced. The circuits reach sub-mW operation which is suitable for ultra-low power applications.



## References

- [1] Y. Hwang and H. Yoo, "A Low Power Folded RF Front-End with Merged LNA and Mixer for ZigBee/Bluetooth", IEEE Radio and Wireless Symposium, pp. 85-86, USA, 2007. DOI: 10.1109/RWS.2007.351737
- [2] F. Haddad, et al., "Sub-1mW RF Voltage Controlled Oscillator Design Optimization for IoT", IEEE Mediterranean Microwave Conference MMS, France, 2017. DOI: 10.1109/MMS.2017.8497152
- [3] P. Neeraja, G. Lakshmana Kumar Moganti and S. Khan Md, "Review of Ultra Low Power Receiver Front-end Designs", International Symposium on Advanced Electrical and Communication Technologies, 2021. DOI: 10.1109/ISAECT53699.2021.9668518
- [4] E. Kargaran, D. Manstretta, and R. Castello, "A Sub-IV, 72  $\mu$ W Stacked LNA-VCO for Wireless Sensor Network Applications", Conf. Research in Microelectronics and Electronics PRIME, 2018. DOI: 10.1109/PRIME.2018.8430306
- [5] Z. Wang and Z. Li, "A 1V 830 $\mu$ W full-band ZigBee receiver front-end with current-reuse and Gm-boosting techniques", IEEE International New Circuits and Systems Conference NEWCAS, 2015. DOI: 10.1109/NEWCAS.2015.7182015
- [6] H. Sjoland, A. Karimi-Sanjaani and A.A. Abidi, "A Merged CMOS LNA and Mixer for a WCDMA Receiver", IEEE Journal of Solid-State Circuits, vol. 38, pp. 1045-1050, June 2003. DOI: 10.1109/JSSC.2003.811952
- [7] W. To-Po, et al., "A low-power oscillator mixer in 0.18  $\mu$ m CMOS technology", IEEE Transactions on Microwave Theory and Techniques, vol. 54, no.1, pp. 88-95, 2006. DOI: 10.1109/TMTT.2005.861671
- [8] M. Pontón, A. Herrera and A. Suárez, "Analysis and design of a concurrent dual-band self-oscillating mixer", International Microwave Symposium (IMS), 2020. DOI: 10.1109/IMS30576.2020.9223855
- [9] S. S. K. Ho and C. E. Saavedra, "A Low-Noise Self-Oscillating Mixer Using a Balanced VCO Load", IEEE Transactions on Circuits and System I: regular papers, vol. 58, no. 8, 2011. DOI: 10.1109/TCSL.2011.2106050
- [10] A. Liscidini, et al., "Single-Stage Low-Power Quadrature RF Receiver Front-End: The LMV Cell", IEEE Journal of Solid-State Circuits, vol. 41, no. 12, pp. 2832-2841, 2006. DOI: 10.1109/JSSC.2006.884824
- [11] C. Elena de, A. Suarez, and S. Sancho, "Envelope transient analysis of self-oscillating mixers", IEEE Transactions on Microwave Theory and Techniques, vol. 52, no. 4, pp. 1090-1100, 2004. DOI: 10.1109/TMTT.2004.825708
- [12] I. Ghorbel, et al., "Ultra-Low-Power Wideband NMOS LC-VCO Design for Autonomous Connected Objects", Analog Integrated Circuits and Signal Processing, Springer, vol. 106, pp. 375-383, 2021. DOI: 10.1007/s10470-020-01613-0
- [13] B. Gilbert, "A precise four-quadrant multiplier with subnanosecond response", IEEE Journal of Solid-State Circuits, vol. 3, pp. 365-373, 1968. DOI: 10.1109/JSSC.1968.1049925
- [14] M. Sironen, Y. Qian, and T. Itoh, "A subharmonic self-oscillating mixer with integrated antenna for 60-GHz wireless applications", IEEE Trans. Microwave Theory Tech., vol. 49, no. 3, pp. 442-450, Mar. 2001. DOI: 10.1109/22.910547
- [15] S.-C. Yen and T.-H. Chu, "A retro-directive antenna array with phase conjugation circuit using subharmonically injection-locked self-oscillating mixers", IEEE Trans. Antennas Propagat., vol. 52, no. 1, pp. 154-164, Jan. 2004. DOI: 10.1109/TAP.2003.822436
- [16] W. Choi, C. Cheon, and Y. Kwon, "A V-band MMIC self oscillating mixer active integrated antenna using a push-pull patch antenna", IEEE Int. Microwave Symp., 2006, pp. 630-633. DOI: 10.1109/MWSYM.2006.249692
- [17] S. Ho and C. Saavedra, "A CMOS broadband low-noise mixer with noise cancellation", IEEE Trans. Microwave Theory Tech., vol. 58, no. 5, pp. 1126-1132, May 2010. DOI: 10.1109/TMTT.2010.2045568
- [18] S. Ho and C. Saavedra, "A low-noise self-oscillating mixer using a balanced VCO load", IEEE Trans. Circuits Syst. I, Reg. Papers, vol. 58, no. 8, pp. 1705-1712, Aug. 2011. DOI: 10.1109/TCSI.2011.2106050
- [19] F. Starzer, H. Forstner, L. Maurer, and A. Stelzer, "A 21-GHz self oscillating down-converter mixer", in Proc. IEEE Topical Meeting Silicon Monolithic Integrated Circuits RF System, Jan. 2012, pp. 93-96. DOI: 10.1109/SiRF.2012.6160148
- [20] T.-P. Wang, C.-C. Chang, R.-C. Liu, M.-D. Tsai, K.-J. Sun, Y.-T. Chang, L.-H. Lu, and H. Wang, "A low-power oscillator mixer in 0.18- $\mu$ m CMOS technology", IEEE Trans. Microwave Theory Tech., vol. 54, no. 1, pp. 88-95, Jan. 2006. DOI: 10.1109/TMTT.2005.861671
- [21] B. R. Jackson and C. E. Saavedra, "A dual-band self-oscillating mixer for C-band and X-band applications", IEEE Trans. Microwave Theory Tech., vol. 58, no. 2, pp. 318-323, Feb. 2010. DOI: 10.1109/TMTT.2009.2037865
- [22] D. Martynenko, G. Fischer, and O. Klymenko, "Implementation of the ultra-low power load-independent LC-VCO", IEEE International Conference on Circuits and Systems (ICCAS), pp. 27-31, 2012. DOI: 10.1109/ICCircuitsAndSystems.2012.6408299
- [23] B. Razavi, "RF Microelectronics", 2nd Edition, Prentice Hall Communications Engineering and Emerging Technologies Series: Prentice Hall Press, 2011.
- [24] S. Shekhar, J. S. Walling, S. Aniruddhan and D. J. Allstot, "CMOS VCO and LNA Using Tuned-Input Tuned-Output Circuits", Journal of Solid-State Circuits, Vol. 43, no. 5, pp. 1177-1184, 2008. DOI: 10.1109/JSSC.2008.920360
- [25] H. Kraïmia, T. Taris, J.-B. Begueret and Y. Deval, "An ultra-low power self-oscillating mixer for WSN applications", European Microwave Conference, 2013. DOI: 10.23919/EuMC.2013.6686783

## Contribution of Individual Authors to the Creation of a Scientific Article (Ghostwriting Policy)

The authors equally contributed in the present research, at all stages from the formulation of the problem to the final findings and solution.

## Sources of Funding for Research Presented in a Scientific Article or Scientific Article Itself

No funding was received for conducting this study.

## Conflicts of Interest

The authors have no conflicts of interest to declare that are relevant to the content of this article.

## Creative Commons Attribution License 4.0 (Attribution 4.0 International, CC BY 4.0)

This article is published under the terms of the Creative Commons Attribution License 4.0

[https://creativecommons.org/licenses/by/4.0/deed.en\\_US](https://creativecommons.org/licenses/by/4.0/deed.en_US)